ARTICLE

Extraction of Viral Nucleic Acids with Carbon Nanotubes Increases SARS-CoV-2 Quantitative Reverse Transcription Polymerase Chain Reaction Detection Sensitivity

Sanghwa Jeong, Eduardo González-Grandío, Nicole Navarro, Rebecca L. Pinals, Francis Ledesma, Darwin Yang, and Markita P. Landry*

Read Online

ACCESS | Metrics & More | Article Recommendations | SI Supporting Information

ABSTRACT: The global SARS-CoV-2 coronavirus pandemic has led to a surging demand for rapid and efficient viral infection diagnostic tests, generating a supply shortage in diagnostic test consumables including nucleic acid extraction kits. Here, we develop a modular method for high-yield extraction of viral single-stranded nucleic acids by using "capture" ssDNA sequences attached to carbon nanotubes. Target SARS-CoV-2 viral RNA can be captured by ssDNA-nanotube constructs *via* hybridization and separated from the liquid phase in a single-tube system with minimal chemical reagents, for downstream quantitative reverse transcription polymerase chain reaction (RT-qPCR) detection. This nanotube-based extraction method enables 100% extraction yield of target SARS-CoV-2 RNA from phosphate-buffered saline in comparison to ~20% extraction yield when using a commercial silica-column kit. Notably, carbon nanotubes enable extraction of nucleic acids directly from 50% human saliva with a similar efficiency as achieved with commercial DNA/RNA extraction kits, thereby bypassing the need for further biofluid purification and avoiding the use of commercial extraction kits. Carbon nanotube-based extraction of viral nucleic acids facilitates high-yield and high-sensitivity identification of viral nucleic acids such as the SARS-CoV-2 viral genome with a reduced reliance on reagents affected by supply chain obstacles.

KEYWORDS: viral diagnostics, qPCR, DNA/RNA extraction, carbon nanotubes, nanotechnology, nanosensors
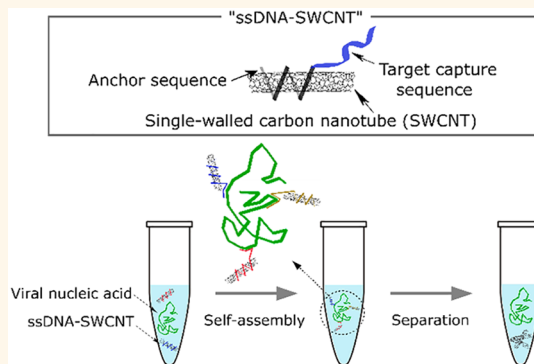
The emergence of the novel human coronavirus (SARS-CoV-2) in late 2019 rapidly escalated into a global pandemic. The high transmission rate and high proportion of asymptomatic infections has led to a massive, global demand for rapid and efficient viral infection diagnostic tests.[1,2] The coronavirus pandemic has unearthed limitations of our diagnostics including insufficient supply, throughput, and variable accuracy, exacerbated by pipeline limitations in accessing reagents, specialized equipment, and trained personnel to conduct tests.[2] Low testing throughput and capacity has resulted in corresponding delays in patients receiving their testing results and cripples contact tracing efforts.[3,4] The two main types of diagnostic tests for virus infections, including SARS-CoV-2, are nucleic acid amplification tests (NAATs) and serological tests. NAATs are currently the gold standard, mainly using real-time reverse transcription polymerase chain reaction (RT-qPCR).[3−6] NAATs can determine whether a

person has an active infection and enable highly sensitive and quantitative diagnosis of infectious diseases. For PCR-based tests, pathogenic nucleic acid extraction from patient samples is required. However, extracting nucleic acids from a patient's biofluid is a complicated and time-consuming task that requires trained technicians to perform, involving many processing steps.[3,4,6] Additionally, specialized materials such as spin columns with silica membranes or magnetic beads and chemically toxic reagents for lysis, binding, washing, and elution are needed. Together with supply chain limitations for

aforementioned reagents, viral nucleic acid extraction constitutes a major bottleneck in current SARS-CoV-2 testing.[1] An advanced and simplified extraction methodology could increase diagnostic availability and efficiency, benefiting patient care and infection control.

Several modified protocols have been developed for extraction of nucleic acids for RT-qPCR, including a chemically driven phenol/chloroform extraction method and solid-phase extraction techniques based on nucleic acid-adsorbing substrates such as silica and cellulose.[7] For example, Wang *et al.* reported a DNA extraction protocol for PCR-based detection by using positively charged polyacrylamide microspheres to adsorb the negatively charged DNA and remove other patient biomolecules.[8] Kolluri *et al.* reported a portable nucleic acid extraction protocol from whole blood with a paper-and-plastic device for capture and purification of nucleic acids on a glass fiber membrane, followed by treatment with a chromatography paper waste pad.[9] In addition to these total nucleic acid extraction methods, affinity-based nucleic acid extraction has been also investigated by using complementary DNA or RNA sequences as capturing ligands. Selective isolation of mRNA from eukaryotic cells is commercially available with the basis of hybridization of a (dT) oligo on magnetic bead matrices to capture mRNA with an oligo (dA) tail. The magnetic beads complexed with mRNAs are next separated from total RNA and genomic DNA with application of a strong magnetic field.[10] Gopal *et al.* reported selective extraction of parasite *Onchocerca volvulus* DNA from the black fly by using magnetic beads with sequence-specific oligonucleotides to capture and immobilize the parasite DNA.[11] In this work, biotinylated capture oligonucleotides were bioconjugated with streptavidin-coated magnetic beads, and this oligonucleotide-based magnetic bead method improved the efficiency of pool screening of black fly vectors. In a similar method, Hei *et al.* published the purification of gRNA of SARS-CoV with magnetic beads modified with capturing oligonucleotides.[12] While selective nucleic acid extraction with complementary DNA/RNA ligands could improve the sensitivity of downstream PCR assays for viral detection by enriching target viral nucleic acids over host DNA and RNA, the aforementioned assays have not replaced or been incorporated into RT-qPCR workflows owing to their complexity, lower sensitivity, cost, or incompatibility with standard RT-qPCR protocols.

Single-walled carbon nanotubes (SWCNT) are one-dimensional, cylindrically shaped allotropes of carbon nanostructures with a high surface area and large aspect ratio due to their unique small diameter of ~1 nm and long lateral dimension up to several micrometers.[13] Colloidal SWCNT dispersions can be prepared by the self-assembly of amphiphilic biopolymers such as nucleic acids and peptides on SWCNT surface *via* $\pi-\pi$ stacking interactions between the aromatic bases of nucleic acids and the sp^2 hybridized SWCNT lattice, avoiding the need for chemical conjugation of ligands to SWCNT. As such, single-stranded DNA (ssDNA) ligands can be adsorbed to SWCNT in helical configurations *via* a quick few-minute probe tip sonication,[14] avoiding time-consuming and relatively costly site-specific attachment chemistries needed to attach ssDNA to most other nanoparticles. Following noncovalent conjugation of ssDNA to SWCNT, the ssDNA on the SWCNT surface is available to hybridize and attach a target oligonucleotide with a complementary sequence, where this hybridization event can

be identified with a change in the ssDNA-SWCNT fluorescence signal.[15]

Herein, we develop a high-yielding method for extraction of viral single-stranded nucleic acids based on ssDNA-SWCNT constructs modified with 10 unique capturing ssDNA sequences that can bind to target nucleic acids. These ssDNA-SWCNT constructs can be readily incorporated into commercial RT-qPCR testing workflows and can either increase the extraction yield of purified target nucleic acids from ~20% (commercial kit) to ~100% (SWCNT-based protocol) or can enable extraction of target nucleic acids in crude patient saliva biofluids, the latter of which avoids the need to purify patient biofluid samples. This viral nucleic extraction protocol permits identification of viral nucleic acids (i) with high nucleic acid extraction yield in complex biofluids, such as unprocessed saliva samples, (ii) without reliance on reagents affected by supply chain obstacles, and (iii) with rapid extraction time.

RESULTS AND DISCUSSION

To enable high-sensitivity extraction of viral nucleic acids, we implemented SWCNT as capture agents for target viral nucleic acids. SWCNTs were designed to enable (1) complexation with target viral nucleic acids *via* sequence-specific capture oligonucleotides on ssDNA-SWCNT constructs and (2) acid precipitation of SWCNT constructs postcapture of target viral nucleic acid (Figure 1). The 10 unique ssDNA capture oligonucleotide sequences are adhered to SWCNT *via* (GT)$_{15}$ anchoring segments, whereby the 10 unique sequences are complementary to different segments of the SARS-CoV-2 viral RNA genome and based on known PCR sequences currently used for PCR detection of SARS-CoV-2 viral RNA (full DNA capture sequences listed in Table 1). Each colloidal ssDNA-SWCNT construct was prepared by probe tip sonication of HiPCo SWCNT and one of the 10 unique capture sequences. Of the capture sequences, nine were chosen to enable hybridization of SWCNT to the nucleocapsid (N) gene region (target 2 to target 10 DNA sequences), and one DNA sequence for the oligo (dA) tail (target 1 DNA sequence). These constructs demonstrate long-term colloidal stability, with negligible ssDNA desorption from the SWCNT surface 72 h after preparation and storage at ambient conditions (Figure S1), enabling their long-term use post-synthesis. Following synthesis, these 10 ssDNA-SWCNT constructs were exposed to the SARS-CoV-2 viral RNA as detailed in several experiments below, to "capture" the viral nucleic acid. We hypothesize that exposing ssDNA-SWCNTs to acidic conditions would neutralize SWCNT surface charges, promoting reversible SWCNT aggregation due to attractive van der Waals interactions and reduced electrostatic repulsive forces. Therefore, the addition of hydrochloric acid (HCl) to the mixture induced precipitation of ssDNA-SWCNT constructs, to which the viral RNA is bound, enabling facile separation of bound viral RNA from the supernatant solution. The precipitates were repeatedly centrifuged and washed with DNase/RNase-free water to remove the unwanted biomolecules. Lastly, the precipitates containing ssDNA-SWCNT constructs and viral RNA were dispersed in phosphate-buffered saline (PBS) and heated to 95 °C to desorb the viral RNA from SWCNT surface. The final PBS solution containing the viral RNA can be directly used for downstream RT-qPCR for viral detection.
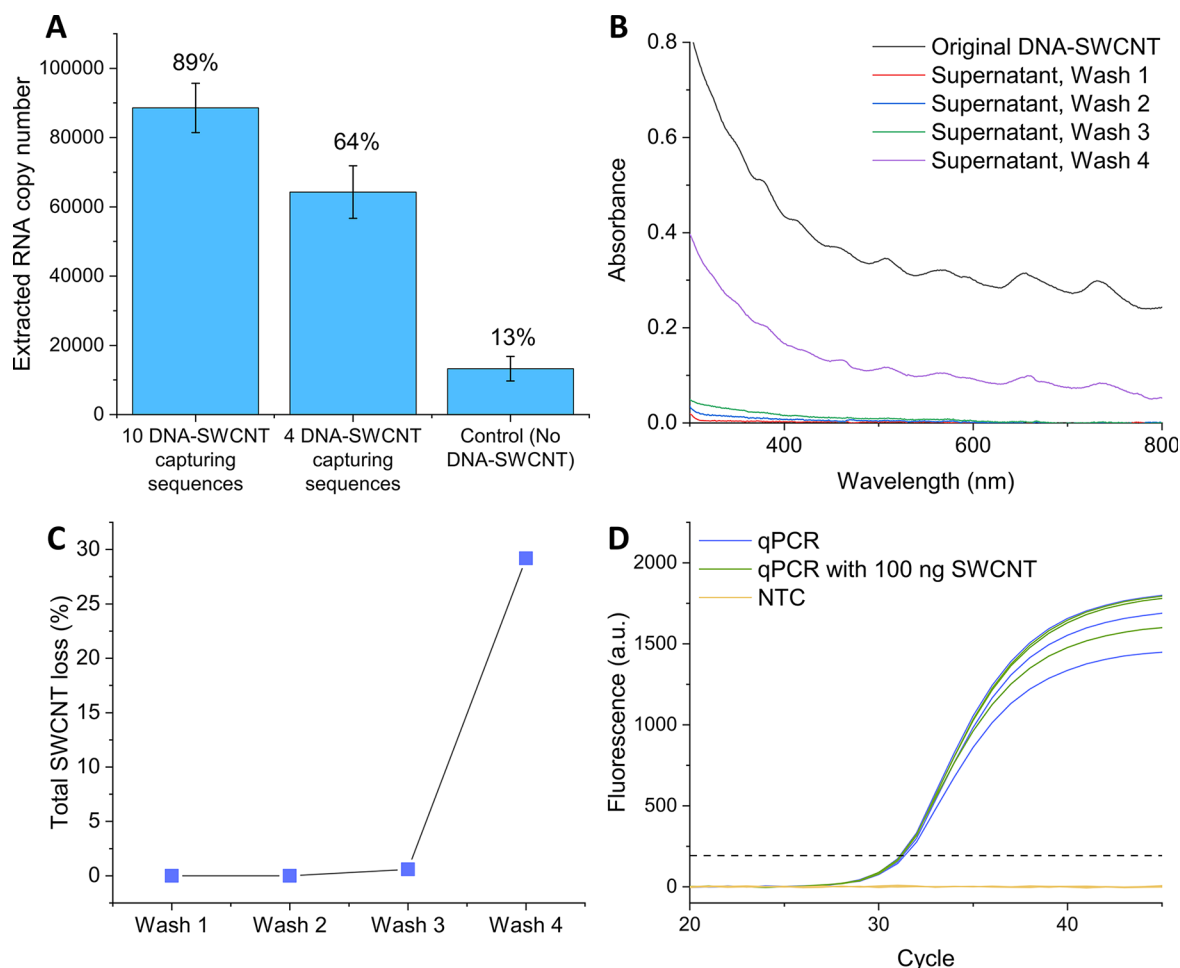
Figure 1. Schematic of single-stranded nucleic acid extraction with ssDNA-SWCNT capturing constructs. (1) Target viral nucleic acid is incubated with ssDNA-functionalized SWCNT capturing constructs, which results in the self-assembly of the target nucleic acid on ssDNA-SWCNTs *via* nucleic acid hybridization. (2) The self-assembled ssDNA-SWCNT and the captured target nucleic acid is precipitated by centrifugation in acidic conditions. (3) The product is purified with nuclease-free water to remove unwanted biomolecules. (4) The product is heated at 95 °C to desorb the target nucleic acids from the SWCNT surface. (5) The extracted target nucleic acids can be amplified by reverse transcription and polymerase chain reaction.

We first optimized the number of unique ssDNA-SWCNT capture sequences to maximize the extraction of SARS-CoV-2 viral RNA. Four $\times 10^6$ copies of synthetic SARS-CoV-2 RNA were spiked into PBS to serve as the RNA standard solution. The RNA from this standard solution was extracted by introducing ssDNA-SWCNT constructs with different capture regions, precipitating, recovering, and detecting the recovered RNA by subsequent RT-qPCR with the corresponding SARS-CoV-2 primer/probe set (Table S2). When four unique

ssDNA-SWCNT constructs (targets 1−4 DNA sequences) were used, 64 ± 8% of the SARS-CoV-2 viral RNA was extracted from the standard solution (Figure 2A). The extraction efficiency was improved to 89 ± 7% when 10 unique ssDNA-SWCNT constructs (targets 1−10 DNA sequences) were used. Conversely, only 13 ± 4% of the viral RNA was recovered in the absence of capturing ssDNA-SWCNT constructs. Based on prior work showing that the number of DNA sequences adsorbed per SWCNT decreases with ssDNA sequence length,[16] we did not increase the number of unique ssDNA target sequences beyond 10 to ensure that SWCNT contained, on average, at least one of each unique capture sequence. We hypothesize that the increase in SARS-CoV-2 viral RNA extraction efficiency with an increased number of unique ssDNA-SWCNT capture sequences is due to the ability of the viral RNA to hybridize with more than one ssDNA-SWCNT construct. Therefore, we propose that when the number of unique capture sequences increases, the viral RNA genome is bound by multiple ssDNA-SWCNT capture sequences and constructs that can be precipitated more easily during the acid precipitation step of the genomic RNA extraction.

To optimize extraction efficiency at the acid precipitation step, we quantified the amount of ssDNA-SWCNT found in the solution supernatant as a function of the number of pellet washes, seeking to maximize the number of washes while minimizing the disturbance of ssDNA-SWCNT from the pellet into the supernatant. To this end, we used $(GT)_{15}$ ssDNA-SWCNT as a model case and quantified the SWCNT concentration in the supernatant by measuring the absorbance of SWCNT at 632 nm (Figure 2B,C). Following the addition of HCl and centrifugation, $(GT)_{15}$-SWCNT was precipitated, and no trace of $(GT)_{15}$-SWCNT was observed in the supernatant. Next, the absorption spectra of the supernatant were monitored following serial supernatant decantation with distilled water. Up to the second water wash, no $(GT)_{15}$-SWCNT was measured in the supernatant, suggesting that two water washes following acid precipitation of ssDNA-SWCNTs is optimal for the acid wash step. Conversely, 0.59% and 29% of $(GT)_{15}$-SWCNT were lost from the pellet and measured in the supernatant following the third and fourth washes, respectively, as the solution became less acidic due to consecutive dilutions. Therefore, for our downstream experiments testing SARS-CoV-2 viral RNA extraction, precipitates were twice-washed during the acid precipitation step to

Table 1. Sequences of ssDNA Used for ssDNA-Functionalized SWCNT Constructs for SARS-CoV-2 RNA Extraction[a]

name	sequence (5′ → 3′)
target 1	GTGTGTGTGTGTGTGTGTGTGTGTGTGTGTTTTTTTTTTTTTTTTTTTTTT
target 2	GTGTGTGTGTGTGTGTGTGTGTGTGTGTCTTAGAAGCCTCAGCAGC
target 3	GTGTGTGTGTGTGTGTGTGTGTGTGTGTTGCGGCCAATGTTTGTAA
target 4	GTGTGTGTGTGTGTGTGTGTGTGTGTGTACTTGATCTTTGAAATTT
target 5	GTGTGTGTGTGTGTGTGTGTGTGTGTGTAGGAAGAAGAGTCACAGT
target 6	GTGTGTGTGTGTGTGTGTGTGTGTGTGTTAAACGGAAAAGCGAAAA
target 7	GTGTGTGTGTGTGTGTGTGTGTGTGTGTTTCTAGCAGGAGAAGTTC
target 8	GTGTGTGTGTGTGTGTGTGTGTGTGTGTTTGAGGAAGTTGTAGCAC
target 9	GTGTGTGTGTGTGTGTGTGTGTGTGTGTGCCCAGTTCCTAGGTAGT
target 10	GTGTGTGTGTGTGTGTGTGTGTGTGTGTTGTCCTCGAGGGAATTTA

[a]From the 5′ end, the $(GT)_{15}$ sequence is for anchoring onto the SWCNT surface, and the subsequent 18-mer sequence is for capturing SARS-CoV-2 RNA.

Figure 2. Optimization of SARS-CoV-2 RNA extraction protocol with ssDNA-SWCNT constructs. (A) RNA extraction efficiency is dependent on the number of unique ssDNA capture sequences used to sequester the target viral RNA. Ten or four DNA-SWCNT capturing sequences denotes targets 1−10 or targets 1−4, respectively, from Table 1. As a control, the extraction protocol is followed without ssDNA-SWCNT. Error bars are standard deviation from $n = 3$ independent trials. (B, C) The loss of $(GT)_{15}$-SWCNT from the precipitated pellet in acidic conditions after multiple washing steps. (B) Absorption spectra of $(GT)_{15}$-SWCNT in the supernatant after each wash step, and (C) total loss of SWCNT calculated from the absorbance of SWCNT at 632 nm, as a function of the number of wash steps. (D) RT-qPCR compatibility of $(GT)_{15}$-SWCNT. RT-qPCR detection of SARS-CoV-2 RNA is unaffected in the presence of 100 ng $(GT)_{15}$-SWCNT in the reaction tube ($n = 3$). NTC = nontemplate control.

minimize the loss of viral RNA but maximize the purity of the recovered nucleic acids.

Prior work has suggested that carbon nanotubes can adversely affect the efficacy of PCR.[17,18] Therefore, we also investigated whether any remaining SWCNT in the final extracted RNA product hinders the subsequent RT-qPCR assay. The standard solution spiked with synthetic SARS-CoV-2 RNA was subject to RT-qPCR to detect the viral RNA, with and without 100 ng of $(GT)_{15}$-SWCNT in the reaction tube, which is equal to the maximum amount of SWCNT used for a single extraction step. The PCR amplification curve revealed only marginal interference of SWCNT constructs on quantitation cycle (C_q) values and curve shapes (Figure 2D), and this result confirms the compatibility of SWCNT for downstream RT-qPCR analysis, in the unlikely event that any were to remain in the supernatant following the acid precipitation and pellet wash step.

The sensitivity of RT-qPCR depends on the efficiency with which the target viral RNA can be extracted. In the case of SARS-CoV-2, the highly variable viral load between individuals motivates extraction of RNA from patient samples (nasal

swabs, saliva samples) with maximal efficiency. Therefore, the synthetic SARS-CoV-2 RNA extraction efficiency of our protocol (Figure 1) was compared to that of a commercial viral RNA/DNA extraction kit (PureLink Viral RNA/DNA Mini Kit, Invitrogen) which uses silica substrates for viral RNA/DNA extraction.[19] To evaluate the extraction efficiency in an inhibitor-free solution, the standard RNA template solution was prepared as described above, by spiking PBS with 2×10^6 copies of synthetic SARS-CoV-2 RNA. Standard solutions were 10-fold serially diluted to probe the working range of nucleic acid copy numbers for extraction. The original spiked RNA samples were also amplified by RT-qPCR without any extraction steps to calculate the baseline RNA recovery yield (Figure 3C). RT-qPCR amplification plots and C_q values of RNA extracted from our method *vs* the PureLink method are shown in Figure 3. Our SWCNT-based extraction protocol recovered ∼100% of the spiked RNA across three logs of spiked RNA concentration ranging from 2×10^3 to 2×10^6 RNA copies per 0.2 mL with a correlation coefficient (R^2) of 0.9917 and an amplification efficiency (E) of 95%. Conversely, the PureLink commercial extraction kit showed a significantly
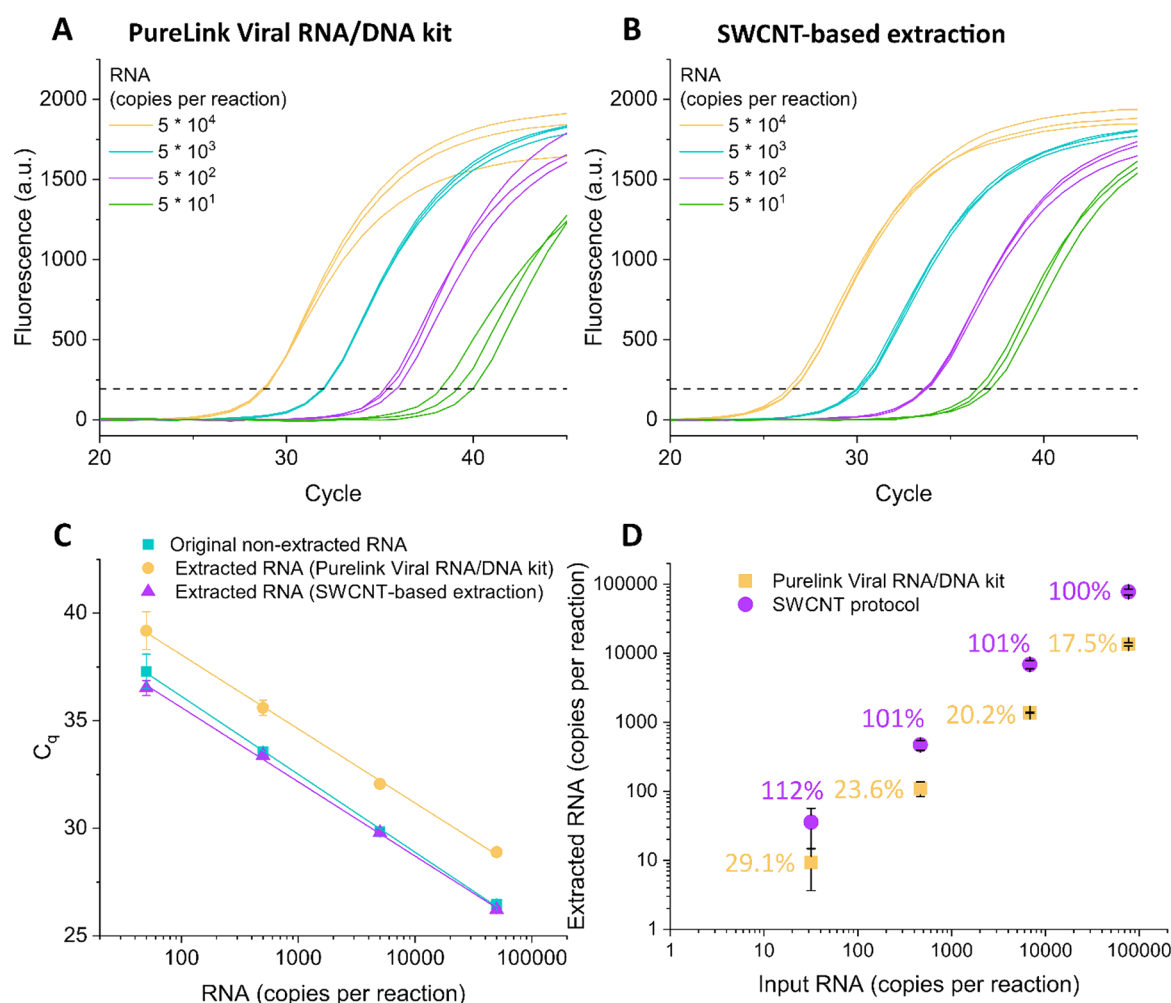
Figure 3. Synthetic SARS-CoV-2 genomic RNA extraction from PBS. RT-qPCR amplification of (A) SARS-CoV-2 RNA extracted by a commercial PureLink Viral RNA/DNA extraction kit and (B) SARS-CoV-2 RNA extracted by ssDNA-SWCNT-based protocol. RNA templates were serially diluted 10-fold across 3 orders of magnitude. (C) Comparison of RT-qPCR amplification of original nonextracted RNA (blue), RNA extracted with ssDNA-SWCNT-based protocol (purple), and RNA extracted with a commercial PureLink Viral RNA/ DNA kit (yellow), where lower C_q values represent better extraction of RNA. (D) Extraction efficiency of RNA in PBS with the ssDNA-SWCNT-based protocol (purple) and PureLink Viral RNA/DNA kit (yellow). Error bars are standard deviation from $n = 3$ independent trials.

lower recovery yield of ∼20% with R^2 of 0.9997 and E of 95%. Both extraction protocols can be completed in 1 h.

A major bottleneck for RT-qPCR-based detection of viral nucleic acids is the necessity to purify a biospecimen prior to PCR detection. Therefore, we sought to compare the extraction efficiency of synthetic SARS-CoV-2 RNA from complex human biofluids with our SWCNT-based protocol *vs* a commercial PureLink kit. To this end, we tested the extraction of SARS-CoV-2 RNA from a 50% (v/v) solution of human saliva in PBS. RT-qPCR amplification and C_q values were obtained as detailed above. Our results show that SWCNT-based extraction protocol enables recovery of >50% of the SARS-CoV-2 synthetic RNA with R^2 of 0.9891 and E of 99% across 3 orders of magnitude of concentration from 2×10^3 to 2×10^6 RNA copies per 0.2 mL. The viral loads of throat swab and sputum in symptomatic patients also range from 1×10^3 to 1×10^6 copies per 0.2 mL.[20] In comparison, the PureLink column-based kit showed a similar recovery yield of >60% with R^2 of 0.9917 and E of 87% (Figure 4). Across all spiked RNA concentrations, we observe a similar RNA recovery efficiency between SWCNT-based *vs* PureLink-

based extractions within the standard deviation of our independent technical replicates. Additionally, as an internal control to ensure the PCR test is run successfully, we confirmed that both SWCNT-based and PureLink-based protocols enable extraction of RNase P RNA from 50% human saliva (Figure S2). Notably, the PureLink kit relies on supply chain limited reagents and requires 15 steps with four tubes to enable extraction of RNA, whereas, SWCNT-based viral RNA extraction can be done as a "one-pot" protocol in a single tube. Therefore, viral RNA can be directly extracted and PCR-quantified from crude human saliva biofluids with our SWCNT-based protocol, at efficiencies comparable to RNA extraction with commercial DNA/RNA extraction kits.

CONCLUSIONS

The ability to first extract and next quantify viral nucleic acids from patients forms the foundation of testing and tracking viral infections, such as that for the current SARS-CoV-2 pandemic. Increasing the extraction yield of viral nucleic acids, to do so from crude patient biofluids and with materials and reagents orthogonal to those in commercial DNA/RNA extraction kits,
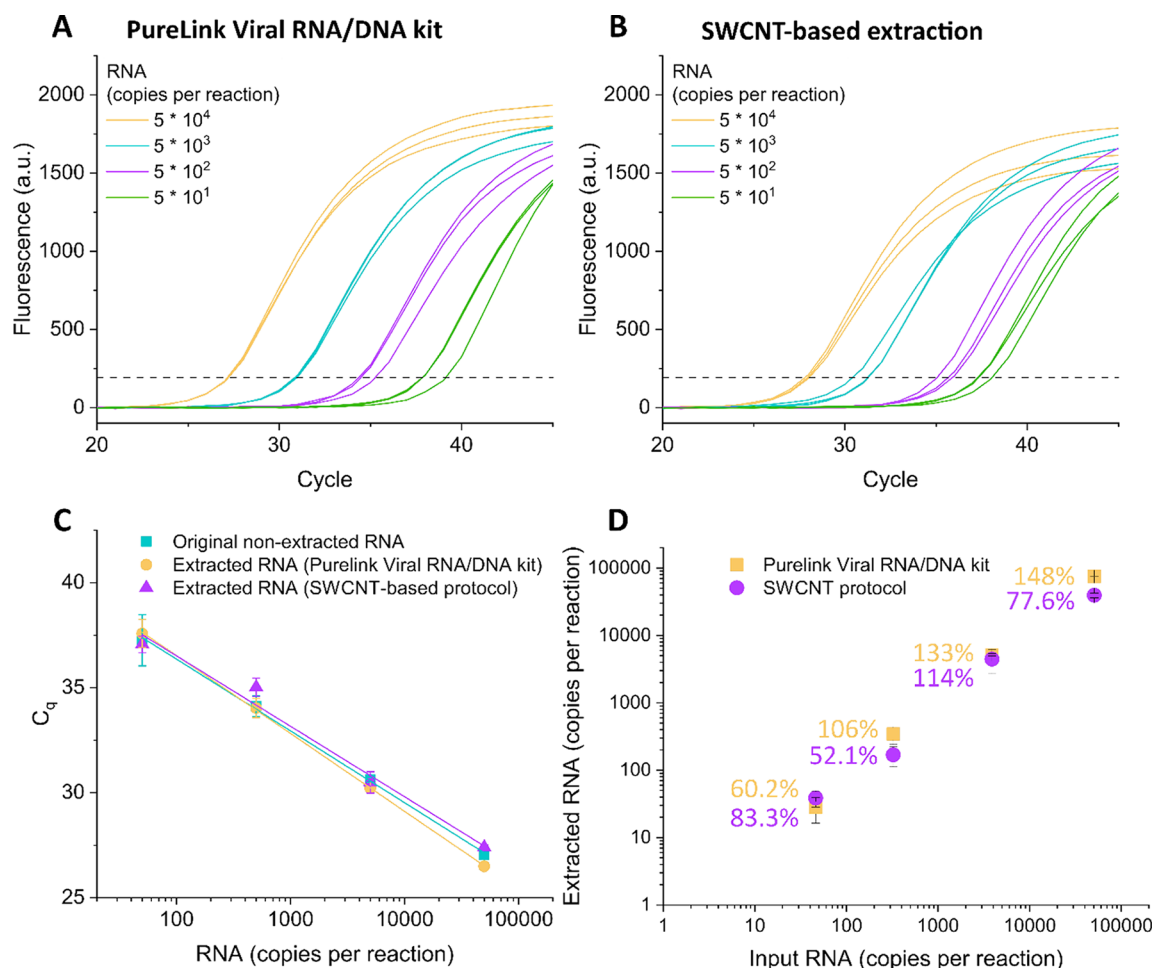
Figure 4. Synthetic SARS-CoV-2 genomic RNA extraction from 50% human saliva. RT-qPCR amplification of (A) SARS-CoV-2 RNA extracted by a commercial PureLink Viral RNA/DNA extraction kit and (B) SARS-CoV-2 RNA extracted by ssDNA-SWCNT-based protocol. RNA was extracted from 50% human saliva spiked with synthetic SARS-CoV-2 genomic RNA. RNA templates were serially diluted 10-fold across 3 orders of magnitude. (C) Comparison of RT-qPCR amplification of original nonextracted RNA (blue), RNA extracted with ssDNA-SWCNT-based protocol (purple), and RNA extracted with a commercial PureLink Viral RNA/DNA kit (yellow). (D) Extraction efficiency of RNA from 50% human saliva with the ssDNA-SWCNT-based protocol (purple) and PureLink Viral RNA/DNA kit (yellow). Error bars are standard deviation from *n* = 3 independent trials.

could greatly increase our testing capacity and could be seamlessly applied to numerous other DNA or RNA detection workflows. In this study, we developed a protocol for extraction of single-stranded viral nucleic acids such as SARS-CoV-2 RNA, for subsequent quantification by RT-qPCR. ssDNA-functionalized SWCNT suspensions with DNA-based "capture" sequences enabled the high-sensitivity extraction of the SARS-CoV-2 RNA from both PBS and human saliva biofluids. To bind the viral nucleic acid to substrates, our SWCNT-based extraction protocol makes use of ssDNA sequences on SWCNT, which contain sequences complementary to specific regions in the SARS-CoV-2 viral genome, serving as capturing ligands. We demonstrate that our SWCNT-based viral RNA extraction protocol enables higher RNA extraction efficiency in PBS (~100% extraction efficiency) as compared to a commercial silica-matrix column PureLink kit (~20% extraction efficiency). Furthermore, we show that SWCNT-based RNA extraction enables us to bypass the lengthy protocols associated with nucleic acid cleanup from patient biofluids by simply mixing ssDNA-SWCNT with human saliva, for facile recovery of viral nucleic acids. Our SWCNT-based extraction protocol combined with the SARS-

CoV-2 CDC RUO kit represented the limit of quantification (LoQ) of 6.4 copies/μL in PBS buffer and LoQ of 9.2 copies/μL in 50% human saliva. In summary, SWCNT-based SARS-CoV-2 viral RNA extraction enables an 80% increase in PCR-based detection sensitivity over the PureLink DNA/RNA extraction kit in PBS and enables similar PCR sensitivity to a commercial kit when viral RNA is extracted from 50% human saliva.

The distinct advantages of our SWCNT-based protocol are in increasing the sensitivity of viral RNA detection down to a LoQ of 6.4 copies/μL in PBS and in enabling RT-qPCR-based viral RNA quantification without silica-column-based purification of patient saliva samples. ssDNA-SWCNTs are produced in a "chemistry-free" system *via* sonication-based conjugation of capturing ssDNA to the SWCNT, greatly reducing the cost and time to prepare this shelf-stable nucleic acid extraction system. Furthermore, the approach described herein requires only small quantities of SWCNT and HCl in a one-pot system. As such, our protocol enables purification of viral nucleic acids directly from patient biofluid, avoiding the need for, and time to operate, silica-matrix columns that require numerous binding, washing, and elution reagents and steps. Lastly, the

modularity of our approach enables the user to choose any specific capturing ssDNA sequences for attachment to SWCNT, potentially enabling detection of different viral nucleic acids. With our approach, simple replacement of the ssDNA capture sequences on the SWCNT could enable a higher sensitivity detection of SARS-CoV-2 variants in which the viral genome has mutated. Similarly, different capture sequences could enable detection of ssDNA-genome-based viruses and positive strand and negative strand RNA viruses.[21,22] We note that the use of SWCNTs for nucleic acid extractions entails deviations from standardized workflows for PCR-based diagnostics, therefore, each new application should examine whether the presence of SWCNTs will interfere with downstream PCR and whether the false positive and false negative test rates are affected.

Taken together, our results demonstrate that ssDNA-SWCNT-based extraction of viral nucleic acids is a modular approach that could serve as a low-cost and rapid method to extract target nucleic acids from patient biofluids. The manufacturing burden and cost of ssDNA-SWCNTs are significantly lower than those associated with current viral nucleic acid extraction kits and protocols, enabling this technology to be potentially implemented in any laboratory with modularity that enables researchers to rapidly substitute their desired capture sequences on the SWCNT for detection of other viral or diagnostic nucleic acids. Future studies should examine whether ssDNA-SWCNT-based extractions enable DNA/RNA recovery for PCR-based tests from true patient samples, to examine whether patient-specific differences and varying viral strains are amenable to this extraction protocol. Pertinent to the current pandemic, this SWCNT-based extraction protocol can alleviate the supply shortages and unprecedented demands for RT-qPCR testing due to its manufacturing simplicity. Lastly, easy substitution of other capture ssDNA on ssDNA-SWCNTs could find applications in the detection of other viral infections such as influenza or in routine clinical diagnostics such as genetic disorder testing using cell-free DNA.

METHODS

Preparation of ssDNA-SWCNT Constructs with Capturing Target Nucleic Acids. For SARS-CoV-2 RNA extraction, 10 unique single-stranded DNA sequences (ssDNAs, purchased from Integrated DNA technologies) were used as viral RNA "capture" sequences, each containing 18-mer DNA sequences complementary to different parts of the SARS-CoV-2 viral RNA genome, and $(GT)_{15}$ "anchor" sequences for adsorption to the SWCNT surface. RNA sequences from SARS-CoV-2 (variant MT007544.1) were used to design the capture ssDNA sequences. Of note, the complementary sequence region can be changed according to the desired target nucleic acid sequences to be recovered. Full ssDNA sequences from target 1 to target 10 are listed in Table 1. For each ssDNA, ssDNA-functionalized SWCNT constructs were generated with the following protocol: 1 mg of HiPCo SWCNT (small diameter HiPCo SWCNT, NanoIntegris) was added to 0.9 mL of PBS, and the solution was mixed with 100 μL of 1 mM ssDNA. The resulting mixture was bath-sonicated for 2 min and probe-tip sonicated for 10 min at 5 W power in an ice bath. After sonication, the ssDNA-SWCNT suspension was centrifuged for 30 min at 16,100g to precipitate unsuspended SWCNT, and the supernatant containing colloidally suspended ssDNA-SWCNT was collected. The supernatant was spin-filtered with a 100 kDa MWCO centrifugal filter at 6000 rpm for 5 min with DNase free water to remove unbound ssDNA, and the purified solution at the top of the filter was collected. This spin filtration to remove unbound ssDNA was repeated three times. The ssDNA-SWCNT suspension was

diluted with PBS buffer and stored at 4 °C until further use. The concentration of the ssDNA-SWCNT suspension was calculated by measuring the absorbance at 632 nm with an extinction coefficient for SWCNT of 0.036 $(mg/L)^{-1}$ cm^{-1}.[23]

Synthetic SARS-CoV-2 Viral RNA Extraction by ssDNA-SWCNT Constructs. Ten unique SARS-CoV-2 RNA-capturing ssDNA-SWCNT suspensions were mixed to make a 1 mg/L ssDNA-SWCNT solution for each unique sequence of ssDNA-SWCNT. The concentration of total ssDNA-SWCNT was 10 mg/L. For the extraction of target RNA from PBS buffer, 190 μL of a known amount of RNA (synthetic SARS-CoV-2 RNA control 1 (MT007544.1), Twist Bioscience) in PBS buffer was mixed with 10 μL of as-prepared total 10 mg/L ssDNA-SWCNT mixture and incubated for 10 min at room temperature to enable target RNA capture by ssDNA-SWCNT constructs. Next, 5 μL of 5 M hydrochloric acid was added to precipitate the ssDNA-SWCNT constructs that had bound target RNA. The solution was gently shaken. The solution was centrifuged at 16,000g for 3 min, and the supernatant was discarded. The precipitates were resuspended in 200 μL DNase/RNase free water. The solution was centrifuged again at 16,000g for 3 min, and the supernatant was discarded. The precipitates were resuspended in 200 μL PBS buffer and briefly sonicated in a bath sonicator (CPX-952-218R, Branson). The mixture solution was incubated at 95 °C for 10 min to weaken the adsorption of nucleic acids from the SWCNT surface. The extracted RNA solution (200 μL) was kept at 4 °C before further use. For downstream RT-qPCR, 5 μL of the extracted RNA solution (2.5% of the total solution) was mixed with the RT-qPCR master mix.

For the extraction of RNA from human saliva, 100 μL of human saliva (pooled normal human saliva, Innovative Research), 85 μL of a known amount of viral RNA in PBS buffer, and 5 μL of 40 U/μL ribonuclease inhibitor (RNaseOUT Recombinant Ribonuclease Inhibitor, Thermo Fisher) were mixed with 10 μL of as-prepared ssDNA-SWCNT mixture and incubated for 10 min at room temperature. Ribonuclease inhibitor was added to prevent degradation of unprotected RNAs in saliva, which can be replaced with viral lysis buffer in the case of a viral specimen test. The remaining PCR protocol is the same as that for nucleic acid extraction from PBS buffer.

For RNA extraction with a commercial PureLink Viral RNA/DNA Mini Kit (Invitrogen), we followed the protocol provided by manufacturer with the proteinase K and carrier RNA included in the kit.

RT-qPCR Protocol. For RT-qPCR, a PCR master mix containing GoTaq 1-Step RT-qPCR System (Promega) Mastermix, 500 nM of forward and reverse primers, 125 nM of FAM-based probes, and 40 U of RNaseOUT Recombinant Ribonuclease Inhibitor (Life Technologies, USA) was used. The sequence details of primers and probes are in Table S2. Five μL of extracted RNA template solution was added in a total volume of 20 μL in triplicate. All reactions were completed in a 96-well plate format (MicroAmp Fast Optical 96-Well Reaction Plate with Barcode, 0.1 mL). The RT-qPCR assays were performed under the following conditions: reverse transcription at 45 °C for 15 min and initial denaturation at 95 °C for 2 min, 45 cycles of denaturation at 95 °C for 3 s, and annealing at 55 °C for 30 s using a standard benchtop real-time thermocycler (CFX96 Touch Real-Time PCR System, BIO-RAD). The C_q values and standard deviations obtained were used to calculate the LoQ. The LoQ was determined with the lowest number of detectable RNA with a coefficient of variation < 35% and was estimated by following conventional calculations.[24]

ASSOCIATED CONTENT

ⓈⒾ Supporting Information

The Supporting Information is available free of charge at https://pubs.acs.org/doi/10.1021/acsnano.1c02494.

Figure S1, Figure S2, Tables S1 and S2; Stability of "capture" ssDNA-SWCNT constructs, RT-qPCR of nucleic acids with human RNase P primer, 10 sequences

targeted in the SARS-CoV-2 viral genome, and primers and probes used for RT-qPCR (PDF)

AUTHOR INFORMATION

Corresponding Author

Markita P. Landry — *Department of Chemical and Biomolecular Engineering and California Institute for Quantitative Biosciences, QB3, University of California, Berkeley, California 94720, United States; Innovative Genomics Institute (IGI), Berkeley, California 94720, United States; Chan Zuckerberg Biohub, San Francisco, California 94158, United States;* orcid.org/0000-0002-5832-8522; Email: landry@berkeley.edu

Authors

Sanghwa Jeong — *Department of Chemical and Biomolecular Engineering, University of California, Berkeley, California 94720, United States; School of Biomedical Convergence Engineering, Pusan National University, Yangsan 50612, Republic of Korea*

Eduardo González-Grandío — *Department of Chemical and Biomolecular Engineering, University of California, Berkeley, California 94720, United States;* orcid.org/0000-0002-2059-4542

Nicole Navarro — *Department of Chemistry, University of California, Berkeley, California 94720, United States*

Rebecca L. Pinals — *Department of Chemical and Biomolecular Engineering, University of California, Berkeley, California 94720, United States;* orcid.org/0000-0002-5369-2317

Francis Ledesma — *Department of Chemical and Biomolecular Engineering, University of California, Berkeley, California 94720, United States;* orcid.org/0000-0002-6280-1394

Darwin Yang — *Department of Chemical and Biomolecular Engineering, University of California, Berkeley, California 94720, United States;* orcid.org/0000-0002-6839-1955

Complete contact information is available at:
https://pubs.acs.org/10.1021/acsnano.1c02494

Author Contributions

S.J. and M.P.L. conceived the idea and designed experiments. S.J., E.G.G., and N.N. performed the experiments and characterized the extraction protocols. All authors discussed the results and wrote the manuscript.

Notes

This paper is based on a previously available preprint: Jeong, S., Grandio, E.G., Navarro, N., Pinals, R., Ledesma, F., Yang, D., Landry, M.P. Extraction of Viral Nucleic Acids with Carbon Nanotubes Increases SARS-CoV-2 RT-qPCR Detection Sensitivity. *medRxiv*. January 26, 2021, ver. 1. 10.1101/2021.01.22.20224675.

The authors declare no competing financial interest.

REFERENCES

(1) Bruce, E. A.; Huang, M.-L.; Perchetti, G. A.; Tighe, S.; Laaguiby, P.; Hoffman, J. J.; Gerrard, D. L.; Nalla, A. K.; Wei, Y.; Greninger, A. L.; Diehl, S. A.; Shirley, D. J.; Leonard, D. G. B.; Huston, C. D.; Kirkpatrick, B. D.; Dragon, J. A.; Crothers, J. W.; Jerome, K. R.; Botten, J. W. Direct RT-qPCR detection of SARS-CoV-2 RNA from Patient Nasopharyngeal Swabs without an RNA Extraction Step. *PLoS Biol.* **2020**, *18*, No. e3000896.

(2) Amen, A. M.; Barry, K. W.; Boyle, J. M.; Brook, C. E.; Choo, S.; Cornmesser, L. T.; Dilworth, D. J.; Doudna, J. A.; Ehrenberg, A. J.; Fedrigo, I.; Friedline, S. E.; Graham, T. G. W.; Green, R.; Hamilton, J. R.; Hirsh, A.; Hochstrasser, M. L.; Hockemeyer, D.; Krishnappa, N.; Lari, A.; Li, H.; et al. Blueprint for a Pop-Up SARS-CoV-2 Testing Lab. *Nat. Biotechnol.* **2020**, *38*, 791−797.

(3) Esbin, M. N.; Whitney, O. N.; Chong, S.; Maurer, A.; Darzacq, X.; Tjian, R. Overcoming the Bottleneck to Widespread Testing: a Rapid Review of Nucleic Acid Testing Approaches for COVID-19 Detection. *RNA* **2020**, *26* (7), 771−783.

(4) Smyrlaki, I.; Ekman, M.; Lentini, A.; Rufino de Sousa, N.; Papanicolaou, N.; Vondracek, M.; Aarum, J.; Safari, H.; Muradrasoli, S.; Rothfuchs, A. G.; Albert, J.; Högberg, B.; Reinius, B. Massive and Rapid COVID-19 Testing Is Feasible by Extraction-Free SARS-CoV-2 RT-PCR. *Nat. Commun.* **2020**, *11* (1), 4812.

(5) Won, J.; Lee, S.; Park, M.; Kim, T. Y.; Park, M. G.; Choi, B. Y.; Kim, D.; Chang, H.; Kim, V. N.; Lee, C. J. Development of a Laboratory-Safe and Low-Cost Detection Protocol for SARS-CoV-2 of the Coronavirus Disease 2019 (COVID-19). *Exp. Neurobiol.* **2020**, *29* (2), 107−119.

(6) Sentmanat, M.; Kouranova, E.; Cui, X. One-Step RNA Extraction for RT-qPCR Detection of 2019-nCoV. *bioRxiv*, October 21, 2020, ver.3. DOI: 10.1101/2020.04.02.022384 (accessed 2021-04-02).

(7) Ali, N.; Rampazzo, R. d. C. P.; Costa, A. D. T.; Krieger, M. A. Current Nucleic Acid Extraction Methods and Their Implications to Point-of-Care Diagnostics. *BioMed Res. Int.* **2017**, *2017*, 9306564.

(8) Wang, J.; Zhang, S.; Xu, X.; Xing, Y.; Li, Z.; Wang, J. Fast DNA Extraction with Polyacrylamide Microspheres for Polymerase Chain Reaction Detection. *ACS Omega* **2020**, *5* (23), 13829−13839.

(9) Kolluri, N.; Albarran, N.; Fan, A.; Olson, A.; Sagar, M.; Young, A.; Gomez-Marquez, J.; Klapperich, C. M. SNAPflex: A Paper-and-Plastic Device for Instrument-Free RNA and DNA Extraction from Whole Blood. *Lab Chip* **2020**, *20*, 3386.

(10) Berensmeier, S. Magnetic Particles for the Separation and Purification of Nucleic Acids. *Appl. Microbiol. Biotechnol.* **2006**, *73* (3), 495−504.

(11) Gopal, H.; Hassan, H. K.; Rodríguez-Pérez, M. A.; Toé, L. D.; Lustigman, S.; Unnasch, T. R. Oligonucleotide Based Magnetic Bead Capture of *Onchocerca volvulus* DNA for PCR Pool Screening of Vector Black Flies. *PLoS Neglected Trop. Dis.* **2012**, *6* (6), No. e1712.

(12) Hei, A.-L.; Cai, J.-P. Development of a Method for Concentrating and Purifying SARS Coronavirus RNA by a Magnetic Bead Capture System. *DNA Cell Biol.* **2005**, *24* (8), 479−484.

(13) Chio, L.; Del Bonis-O'Donnell, J. T.; Kline, M. A.; Kim, J. H.; McFarlane, I. R.; Zuckermann, R. N.; Landry, M. P. Electrostatic Assemblies of Single-Walled Carbon Nanotubes and Sequence-Tunable Peptoid Polymers Detect a Lectin Protein and Its Target Sugars. *Nano Lett.* **2019**, *19* (11), 7563−7572.

(14) Gigliotti, B.; Sakizzie, B.; Bethune, D. S.; Shelby, R. M.; Cha, J. N. Sequence-Independent Helical Wrapping of Single-Walled Carbon Nanotubes by Long Genomic DNA. *Nano Lett.* **2006**, *6* (2), 159−164.

(15) Harvey, J. D.; Jena, P. V.; Baker, H. A.; Zerze, G. H.; Williams, R. M.; Galassi, T. V.; Roxbury, D.; Mittal, J.; Heller, D. A. A Carbon Nanotube Reporter of MicroRNA Hybridization Events *in Vivo*. *Nat. Biomed. Eng.* **2017**, *1* (4), 0041.

(16) Nißler, R.; Mann, F. A.; Chaturvedi, P.; Horlebein, J.; Meyer, D.; Vuković, L.; Kruss, S. Quantification of the Number of Adsorbed DNA Molecules on Single-Walled Carbon Nanotubes. *J. Phys. Chem. C* **2019**, *123* (8), 4837−4847.

(17) Zhang, Z.; Shen, C.; Wang, M.; Han, H.; Cao, X. Aqueous Suspension of Carbon Nanotubes Enhances the Specificity of Long PCR. *BioTechniques* **2008**, *44* (4), 537−545.

(18) Williams, R. M.; Nayeem, S.; Dolash, B. D.; Sooter, L. J. The Effect of DNA-Dispersed Single-Walled Carbon Nanotubes on the Polymerase Chain Reaction. *PLoS One* **2014**, *9* (4), No. e94117.

(19) Sathiamoorthy, S.; Malott, R. J.; Gisonni-Lex, L.; Ng, S. H. S. Selection and Evaluation of an Efficient Method for the Recovery of Viral Nucleic Acids from Complex Biologicals. *npj Vaccines* **2018**, *3* (1), 31.

(20) Pan, Y.; Zhang, D.; Yang, P.; Poon, L. L. M.; Wang, Q. Viral Load of SARS-CoV-2 in Clinical Samples. *Lancet Infect. Dis.* **2020**, *20*, 411−412.

(21) Tran, T. L.; Nguyen, T. T.; Huyen Tran, T. T.; Chu, V. T.; Thinh Tran, Q.; Tuan Mai, A. Detection of Influenza A Virus Using Carbon Nanotubes Field Effect Transistor Based DNA Sensor. *Phys. E* **2017**, *93*, 83−86.

(22) Tam, P. D.; Van Hieu, N.; Chien, N. D.; Le, A.-T.; Anh Tuan, M. DNA Sensor Development Based on Multi-Wall Carbon Nanotubes for Label-Free Influenza Virus (Type A) Detection. *J. Immunol. Methods* **2009**, *350* (1), 118−124.

(23) Zhang, J.; Landry, M. P.; Barone, P. W.; Kim, J.-H.; Lin, S.; Ulissi, Z. W.; Lin, D.; Mu, B.; Boghossian, A. A.; Hilmer, A. J.; Rwei, A.; Hinckley, A. C.; Kruss, S.; Shandell, M. A.; Nair, N.; Blake, S.; Sen, F.; Sen, S.; Croy, R. G.; Li, D.; et al. Molecular Recognition Using Corona Phase Complexes Made of Synthetic Polymers Adsorbed on Carbon Nanotubes. *Nat. Nanotechnol.* **2013**, *8* (12), 959−968.

(24) Forootan, A.; Sjöback, R.; Björkman, J.; Sjögreen, B.; Linz, L.; Kubista, M. Methods to Determine Limit of Detection and Limit of Quantification in Quantitative Real-Time PCR (qPCR). *Biomol. Detect. Quantif.* **2017**, *12*, 1−6.